Supplementary information: Citrate-gel preparation and ammonia synthesis activity of compounds in the quaternary $(Ni,M)_2Mo_3N$ (M = Cu or Fe) systems

Samia Al Sobhi,[a] Justin S. J. Hargreaves,[b,*] Andrew L. Hector[a,*] and Said Laassiri[b]

[a] School of Chemistry, University of Southampton, Highfield, Southampton SO17 1BJ, United Kingdom

[b] WestCHEM, School of Chemistry, University of Glasgow, Joseph Black Building, Glasgow G12 8QQ, United Kingdom

Table S1 Quantities of reagents used in the synthesis of nickel copper molybdenum nitride $(Ni,M)_2Mo_3N$ (M = Cu or Ni).

x in $Ni_{2-x}Cu_xMo_3N$	$Ni(NO_3)_2{\cdot}6H_2O$	$Cu(NO_3)_2{\cdot}3H_2O$	$(NH_4)_6Mo_7O_{24}{\cdot}4H_2O$	Citric acid monohydrate
0.1	2.09 g / 7.19 mmol	0.09 g / 0.37 mmol	2 g / 1.62 mmol	7.94 g / 37.8 mmol
0.2	1.97 g / 6.77 mmol	0.18 g / 0.75 mmol		
0.3	1.86 g / 6.40 mmol	0.27 g / 1.12 mmol		
0.4	1.76 g / 6.05 mmol	0.36 g / 1.49 mmol		
0.5	1.65 g / 5.67 mmol	0.46 g / 1.90 mmol		
0.6	1.54 g / 5.30 mmol	0.55 g / 2.28 mmol		
0.7	1.43 g / 4.92 mmol	0.64 g / 2.65 mmol		
0.75	1.37 g / 4.71 mmol	0.68 g / 2.81 mmol		
0.9	1.21 g / 4.16 mmol	0.82 g / 3.39 mmol		
1.0	1.10 g / 3.78 mmol	0.91 g / 3.77 mmol		
x in $Ni_{2-x}Fe_xMo_3N$	$Ni(NO_3)_2{\cdot}6H_2O$	$Fe(NO_3)_2{\cdot}6H_2O$	$(NH_4)_6Mo_7O_{24}{\cdot}4H_2O$	Citric acid monohydrate
0.1	2.09 g / 7.19 mmol	0.15 g / 0.37 mmol	2 g / 1.62 mmol	7.94 g / 37.8 mmol
0.2	1.97 g / 6.77 mmol	0.31 g / 0.77 mmol		
0.3	1.86 g / 6.40 mmol	0.46 g / 1.14 mmol		
0.4	1.76 g / 6.05 mmol	0.61 g / 1.51 mmol		
0.5	1.65 g / 5.67 mmol	0.76 g / 1.89 mmol		
0.6	1.54 g / 5.30 mmol	0.92 g / 2.28 mmol		
0.7	1.43 g / 4.92 mmol	1.07 g / 2.65 mmol		
0.8	1.37 g / 4.71 mmol	1.22 g / 3.02 mmol		
0.9	1.21 g / 4.16 mmol	1.37 g / 3.39 mmol		
1.0	1.10 g / 3.78 mmol	1.53 g / 3.79 mmol		
1.1	0.99 g / 3.40 mmol	1.68 g / 4.16 mmol		

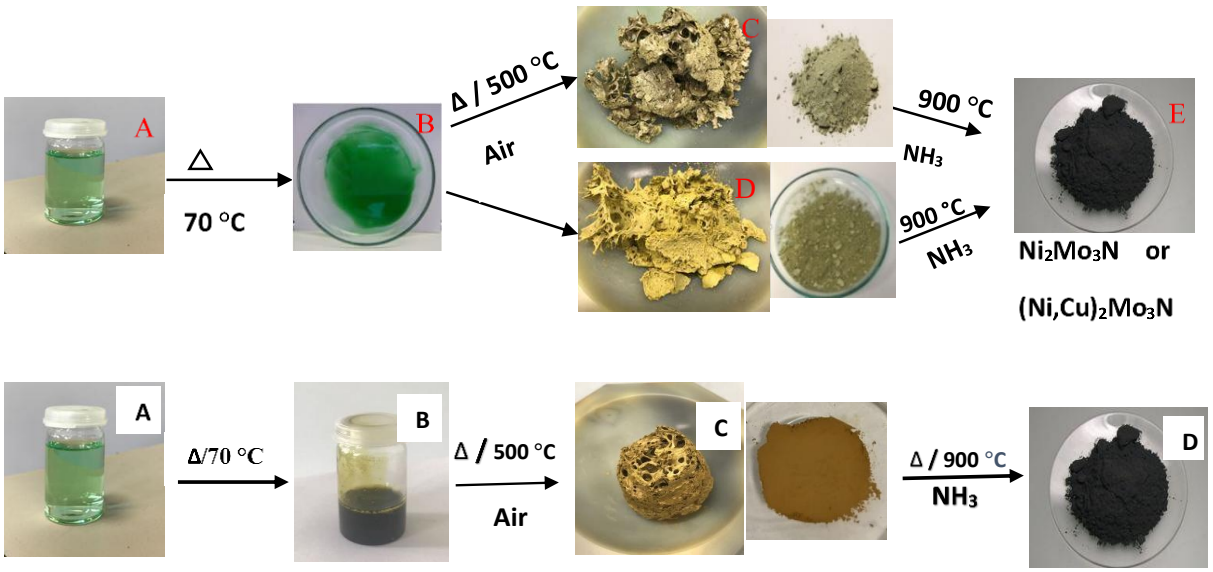

Fig. S1 Schematic description of the citrate-gel process to produce the filled β-manganese type phases, with Ni_2Mo_3N and the $(Ni,Cu)_2Mo_3N$ compounds represented in the top scheme and the $(Ni,Fe)_2Mo_3N$ compounds at the bottom. From left to right: starting solution (green), gel (green or brown) after evaporating, greyish and yellowish foams after heat treatment in air at 500 °C in air, and final fine powder after heating at 900 °C in flowing NH_3.

Note S1 Ammonia production rate calculations

The ammonia produced during catalysis was bubbled through a dilute H2So4 solutions, whose conductivity is known to vary linearly with the acid concentration.

Moles of H_2SO_4 = Concentration (H_2SO_4) × Volume (H_2SO_4) $= 0.001\ \text{mol L}^{-1} \times 0.1\ \text{L} = 1 \times 10^{-4}\text{moles}$

0. 0002 moles of ammonia are required to completely react with H_2SO_4

Change in conductivity for the reaction:

$$H_2SO_4 + 2NH_3 \rightarrow (NH_4)_2SO_4$$

$$= 802.2\ \mu\text{S cm}^{-1} - 332\ \mu\text{S cm}^{-1} = 470\ \mu\text{S cm}^{-1}$$

The calibration value= Number of moles of ammonia required / Total change in conductivity

$$= 2 \times 10^{-4}\ \text{moles} / 470\ \mu\text{Scm}^{-1}$$

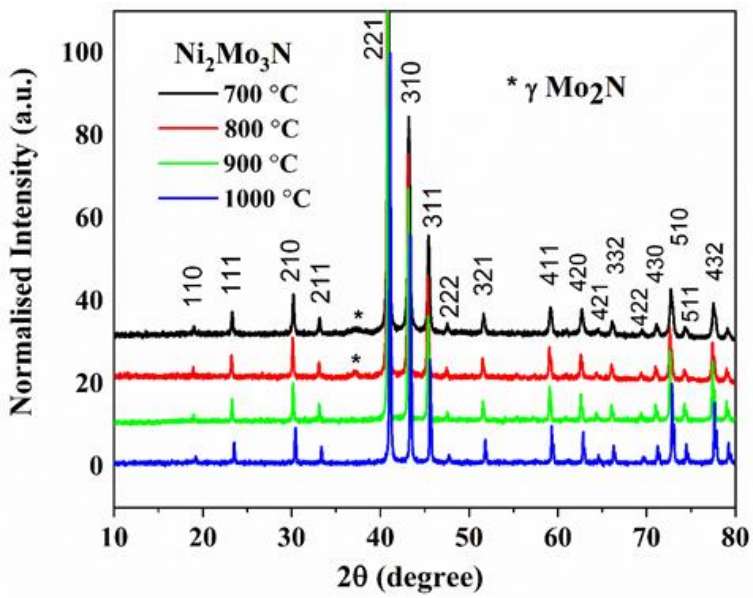

Fig. S2 Powder XRD patterns for Ni_2Mo_3N powder prepared by firing the oxide precursors at 700 °C, 800 °C , 900 °C and 1000 °C under NH_3 gas. The peaks marked with asterisks (*) denote the γ Mo_2N rock- salt as a secondary phase.

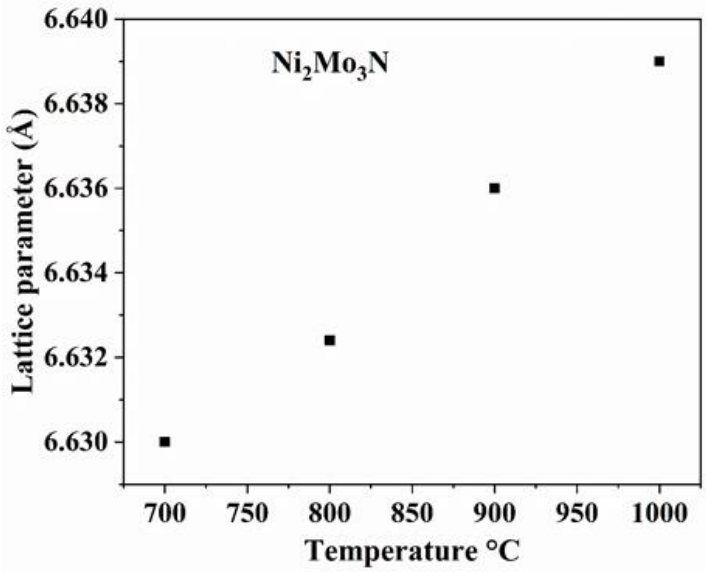

Fig. S3 Firing temperature dependence of the lattice parameter for Ni_2Mo_3N.

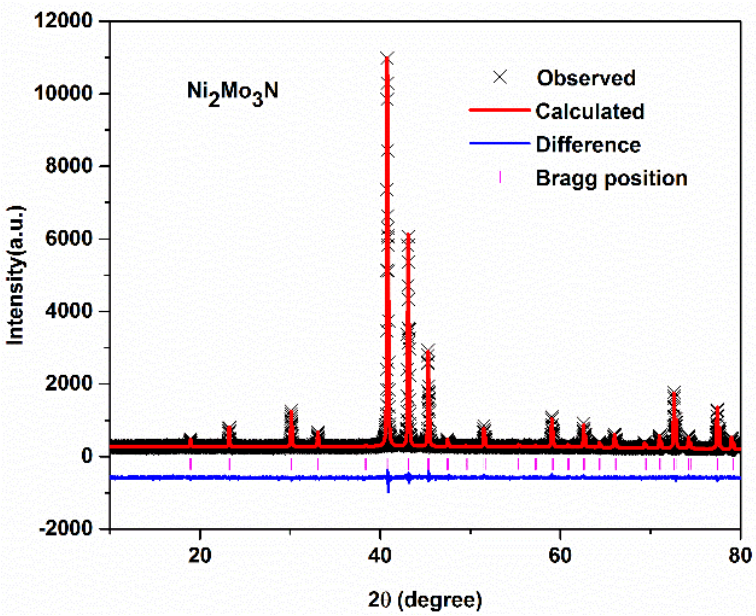

Fig. S4 Rietveld fit to the XRD data of Ni_2Mo_3N. Black crosses mark the data points, the red continuous line the fit and the blue continuous line the difference. Pink tick marks show the positions of the allowed reflections for the filled β-manganese structure in $P4_132$ (R_p = 6.68 %, R_{wp} = 8.66 %, lattice parameter= 6.636(1) Å.

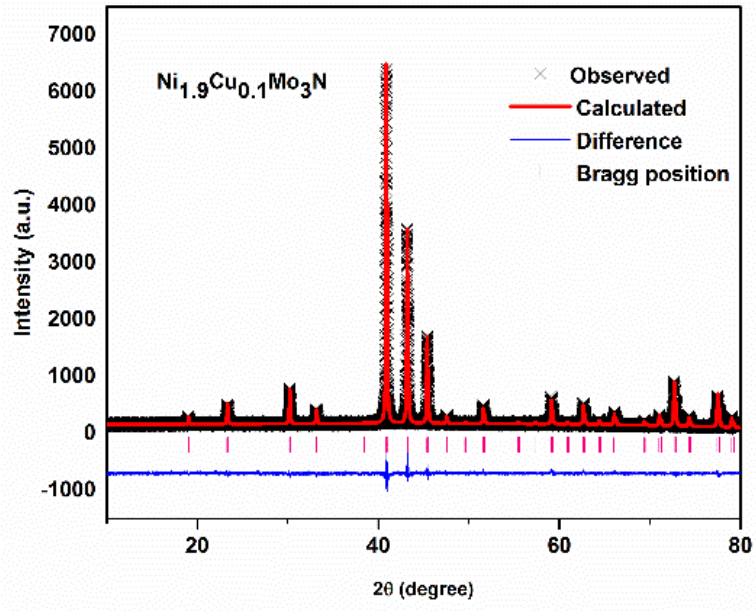

Fig. S5 Rietveld fit to the XRD data of $Ni_{1.9}Cu_{0.1}Mo_3N$. Black crosses mark the data points, the red continuous line the fit and the blue continuous line the difference. Pink tick marks show the positions of the allowed reflections for the filled β-manganese structure in $P4_132$ (R_p = 5.39 %, R_{wp}= 7.03 %, lattice parameter= 6.634036(2)Å

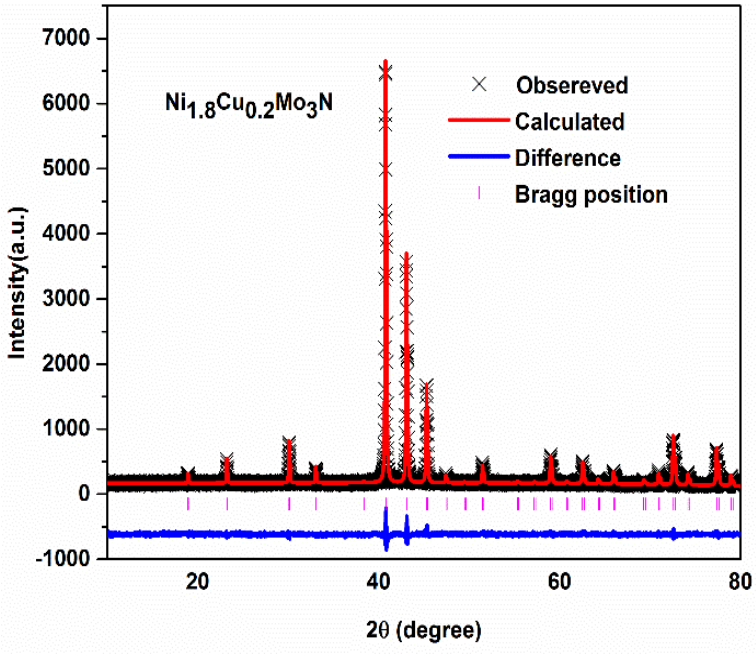

Fig. S6 Rietveld fit to the XRD data of $Ni_{1.8}Cu_{0.2}Mo_3N$. Black crosses mark the data points, the red continuous line the fit and the blue continuous line the difference. Pink tick marks show the positions of the allowed reflections for the filled β-manganese structure in $P4_132$. (R_p = 6.38 %, R_{wp} = 7.98 %, lattice parameter= 6.643(1) Å.

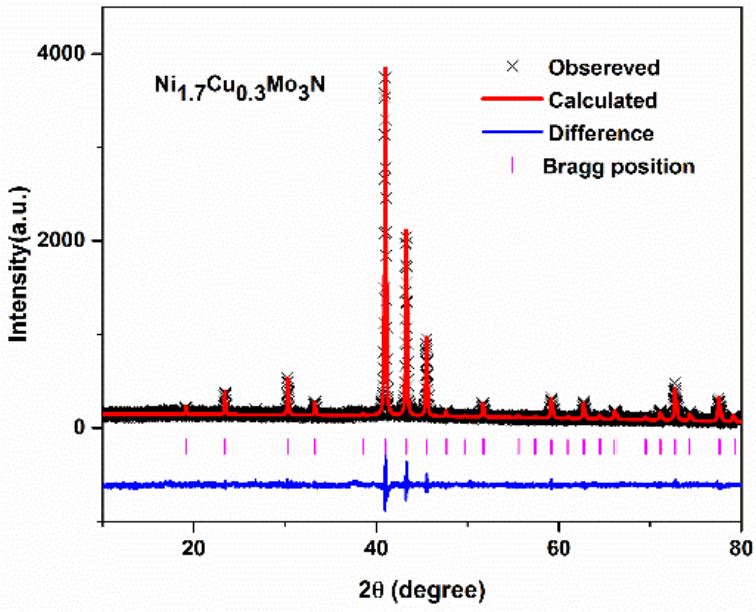

Fig. S7 Rietveld fit to the XRD data of $Ni_{1.7}Cu_{0.3}Mo_3N$. Black crosses mark the data points, the red continuous line the fit and the blue continuous line the difference. Pink tick marks show the positions of the allowed reflections for the filled β-manganese structure in $P4_132$. (R_p = 7.57 %, R_{wp} = 9.49 %, lattice parameter= 6.645(3) Å.

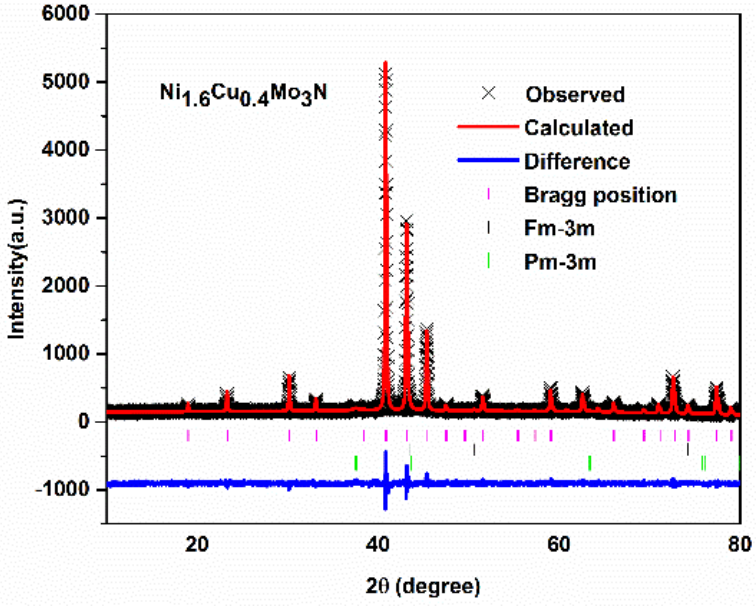

Fig. S8 Rietveld fit to the XRD data of data of $Ni_{1.6}Cu_{0.4}Mo_3N$. Black crosses mark the data points, the red continuous line the fit and the blue continuous line the difference. Pink tick marks show the positions of the allowed reflections for the filled β-manganese structure in $P4_132$. (R_p = 6.12 %, R_{wp} = 7.77 %, wt fraction= 96(2) %, lattice parameter= 6.6447(2) Å, crystallite size= 147(5) nm. Black tick marks represent allowed reflection positions for Cu metal (Fm-3m, wt fraction = 1.3 %, lattice parameter= 3.6(1) Å, (green) tick marks represent allowed reflection positions for γ-Mo_2N (space group: Pm-3m, wt fraction= 2.6 %, lattice parameter = 4.17(3) Å.

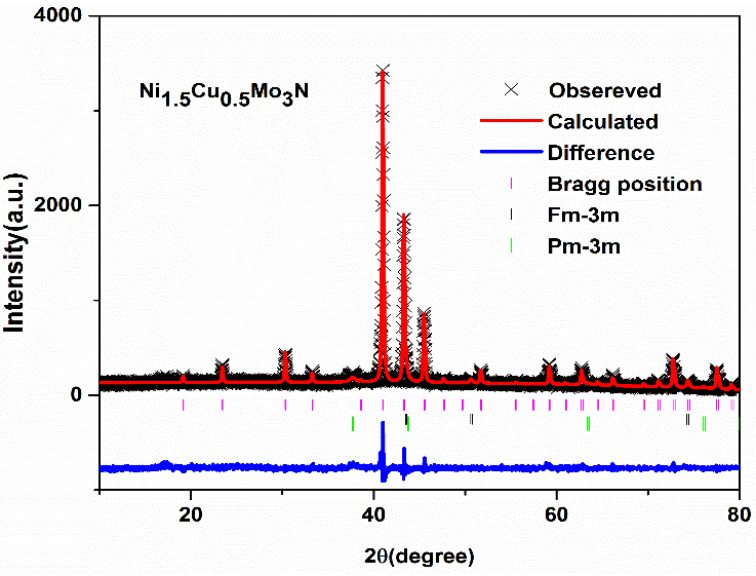

Fig. S9 Rietveld fit to the XRD data of $Ni_{1.5}Cu_{0.5}Mo_3N$. Black crosses mark the data points, the red continuous line the fit and the blue continuous line the difference. Pink tick marks show the positions of the allowed reflections for the filled β-manganese structure in $P4_132$. (R_p = 7.95 %, R_{wp} = 10.28 %, wt fraction= 94.3(3) %, lattice parameter= 6.6445(8) Å, crystallite size= 139(5) nm. Black tick marks represent allowed reflection positions for Cu metal (Fm-3m, wt fraction= 2.5 %, lattice parameter= 3.62(1) Å. Green tick marks represent allowed reflection positions for γ-Mo_2N (Pm-3m, wt fraction =3.2%, lattice parameter= 4.17(2) Å.

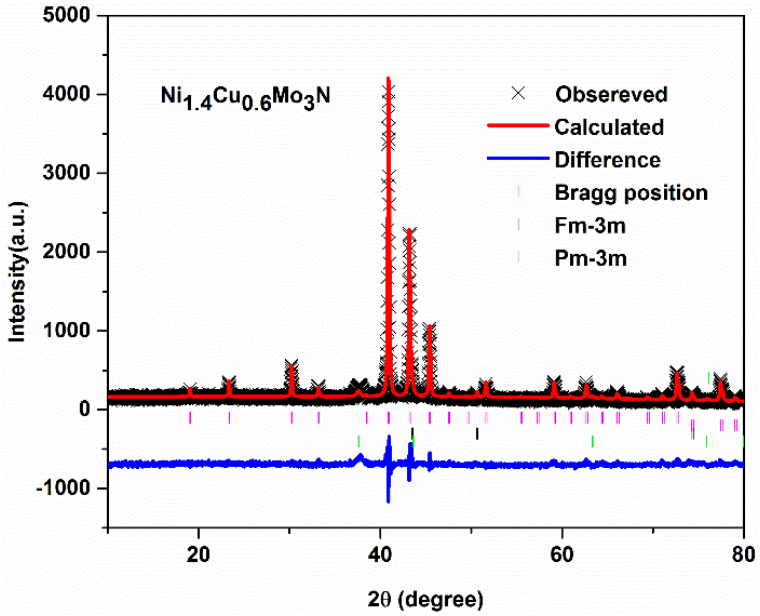

Fig. S10 Rietveld fit to the XRD data of $Ni_{1.4}Cu_{0.6}Mo_3N$. Black crosses mark the data points, the red continuous line the fit and the blue continuous line the difference. Pink tick marks show the positions of the allowed reflections for the filled β-manganese structure in $P4_132$. (R_p = 13.25 %, R_{wp} = 10.2 %, wt fraction= 96(6) %, lattice parameter= 6.6442(4), crystallite size= 116(2) nm. Black tick marks represent allowed reflection positions for Cu metal (Fm-3m, wt fraction= 1.8 %, lattice parameter= 3.62(5) Å. Green tick marks represent allowed reflection positions for γ-Mo_2N (Pm-3m, wt fraction=2.3 %, lattice parameter= 4.167(2) Å.

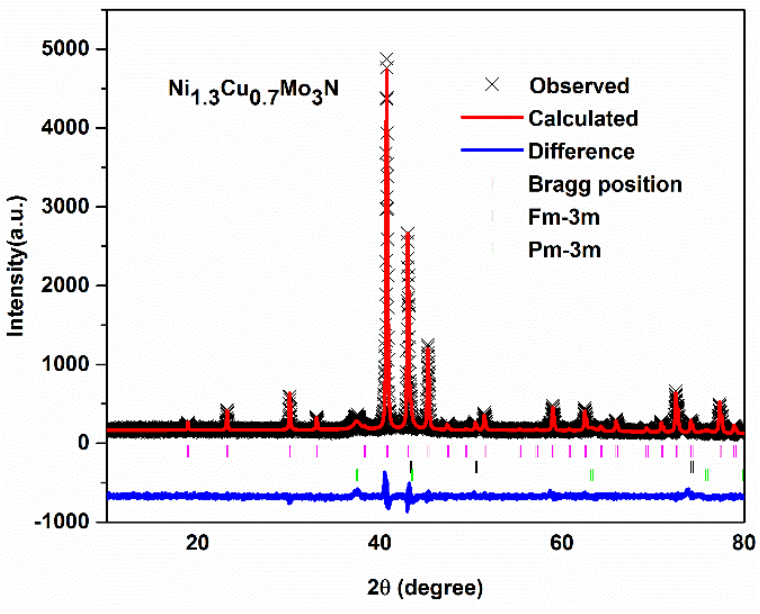

Fig. S11 Rietveld fit to the XRD data of $Ni_{1.3}Cu_{0.7}Mo_3N$. Black crosses mark the data points, the red continuous line the fit and the blue continuous line the difference. Pink tick marks show the positions of the allowed reflections for the filled β-manganese structure in $P4_132$ (R_p = 6.73 %, R_{wp} = 8.90 %, wt fraction= 89.2(8) %, lattice parameter= 6.6441(2) Å, crystallite size= 120(13) nm. Black tick marks represent allowed reflection positions for Cu metal (Fm-3m, wt fraction = 3.5 %, lattice parameter= 3.62 (3) Å. Green tick marks represent allowed reflection positions for γ-Mo_2N (Pm-3m, wt fraction= 7.3 %, lattice parameter= 4.16(1) Å.

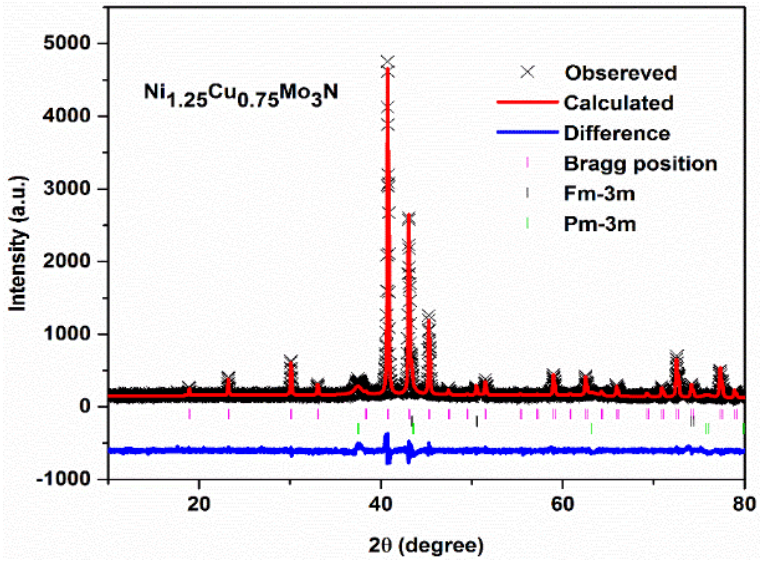

Fig. S12 Rietveld fit to the XRD data of $Ni_{1.25}Cu_{0.75}Mo_3N$. Black crosses mark the data points, the red continuous line the fit and the blue continuous line the difference. Pink tick marks show the positions of the allowed reflections for the filled β-manganese structure in $P4_132$ (R_p = 6.88 %, R_{wp} = 9.03 %, wt fraction= 86(1) %, lattice parameter= 6.6441(2) Å, crystallite size= 120(15) nm. Black tick marks represent allowed reflection positions for Cu metal (Fm-3m, wt fraction= 4.4(2) %, lattice parameter= 3.616(3) Å. Green tick marks represent allowed reflection positions for γ-Mo_2N (Pm-3m, wt fraction= 9.6(3) %, lattice parameter= 4.16(1) Å.

Table S2 Structure information from Rietveld fits for $Ni_{2-x}Cu_x Mo_3N$ series

Composition	a/Å	Ni/ Cu x (8c x, x, x)	Ni/ Cu Uiso / Å²	Mo 12 d (1/8, y, z)			N 4a 3/8, 3/8, 3/8
				y	Z	Uiso/ Å²	Uiso / Å²
Ni_2Mo_3N	6.6364(1)	0.0663(2)	0.0262(8)	0.20176(1)	0.45176(1)	0.02668(5)	0.2500
$Ni_{1.9}Cu_{0.1}Mo_3N$	6.6399(6)	0.06644(1)	0.03452(1)	0.2018(1)	0.4518(1)	0.03345(4)	
$Ni_{1.8}Cu_{0.2}Mo_3N$	6.643(1)	0.06692(4)	0.04099(2)	0.20195(2)	0.45195(2)	0.0425(3)	
$Ni_{1.7}Cu_{0.3}Mo_3N$	6.645(3)	0.0672(4)	0.04385 (2)	0.20222(2)	0.45222(2)	0.04376 (1)	

Table S3 The atom % of the Cu-doped samples from (0-0.3) evaluated by EDX analysis

Element	Ni_2Mo_3N		$Ni_{1.9}Cu_{0.1}Mo_3N$		$Ni_{1.8}Cu_{0.2}Mo_3N$		$Ni_{1.7}Cu_{0.3}Mo_3N$	
	Calculated	**Actual**	**Calculated**	**Actual**	**Calculated**	**Actual**	**Calculated**	**Actual**
Ni	40	36.4	38	36.5	36	32	34	27.9
Cu	0	0	2	1.7	4	2.8	6	4
Mo	60	63	60	61.2	60	65	60	67

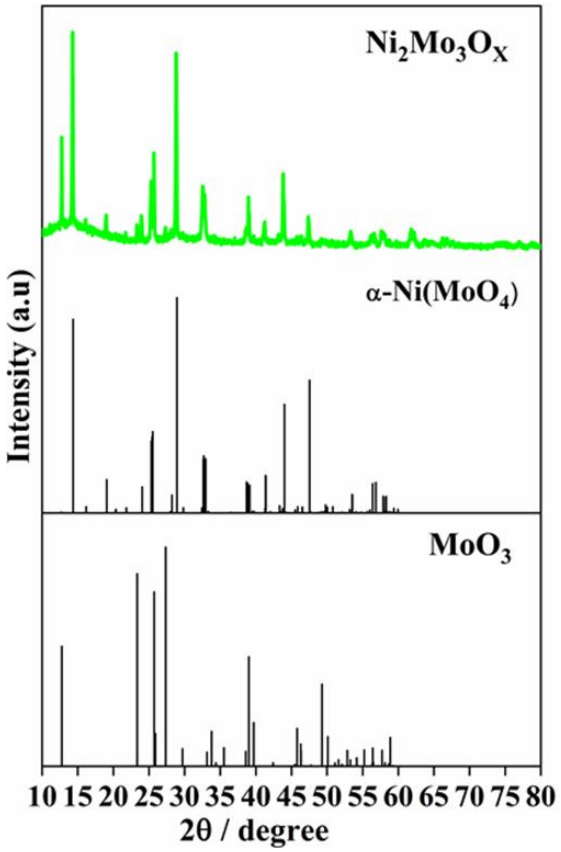

Fig. S13 Powder XRD pattern of the products of heating Ni_2Mo_3N in the TGA to 700 °C in 50% O_2/50% Ar.

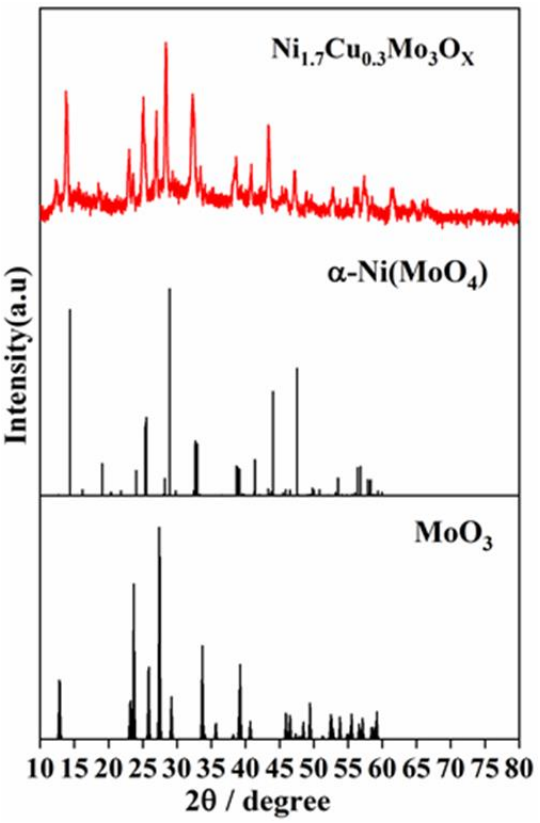

Fig. S14 Powder XRD pattern of the products of heating $Ni_{1.7}Cu_{0.3}Mo_3N$ in the TGA to 700 °C in 50% O_2/50% Ar.

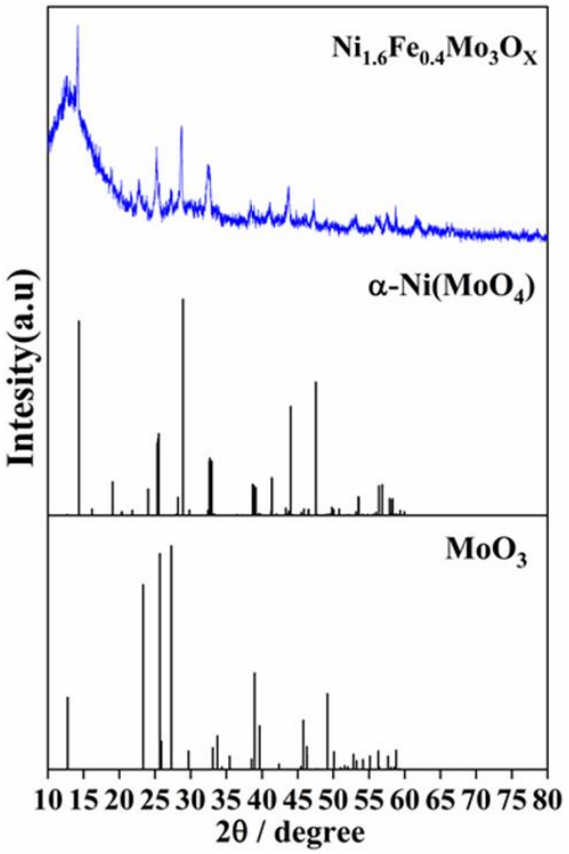

Fig. S15 Powder XRD pattern of the products of heating $Ni_{1.6}Fe_{0.4}Mo_3N$ in the TGA to 700 °C in 50% O_2/50% Ar

Table S4 Mass % of various oxides formed from TGA of the resulting composites

Composition	Overall Mass Gain Observed/ %	Expected Mass Gain/ %
Ni_2Mo_3N	38.30	37.95
$Ni_{1.9}Cu_{0.1}Mo_3N$	37.60	38.10
$Ni_{1.8}Cu_{0.2}Mo_3N$	37.55	38.26
$Ni_{1.7}Cu_{0.3}Mo_3N$	37.45	38.41

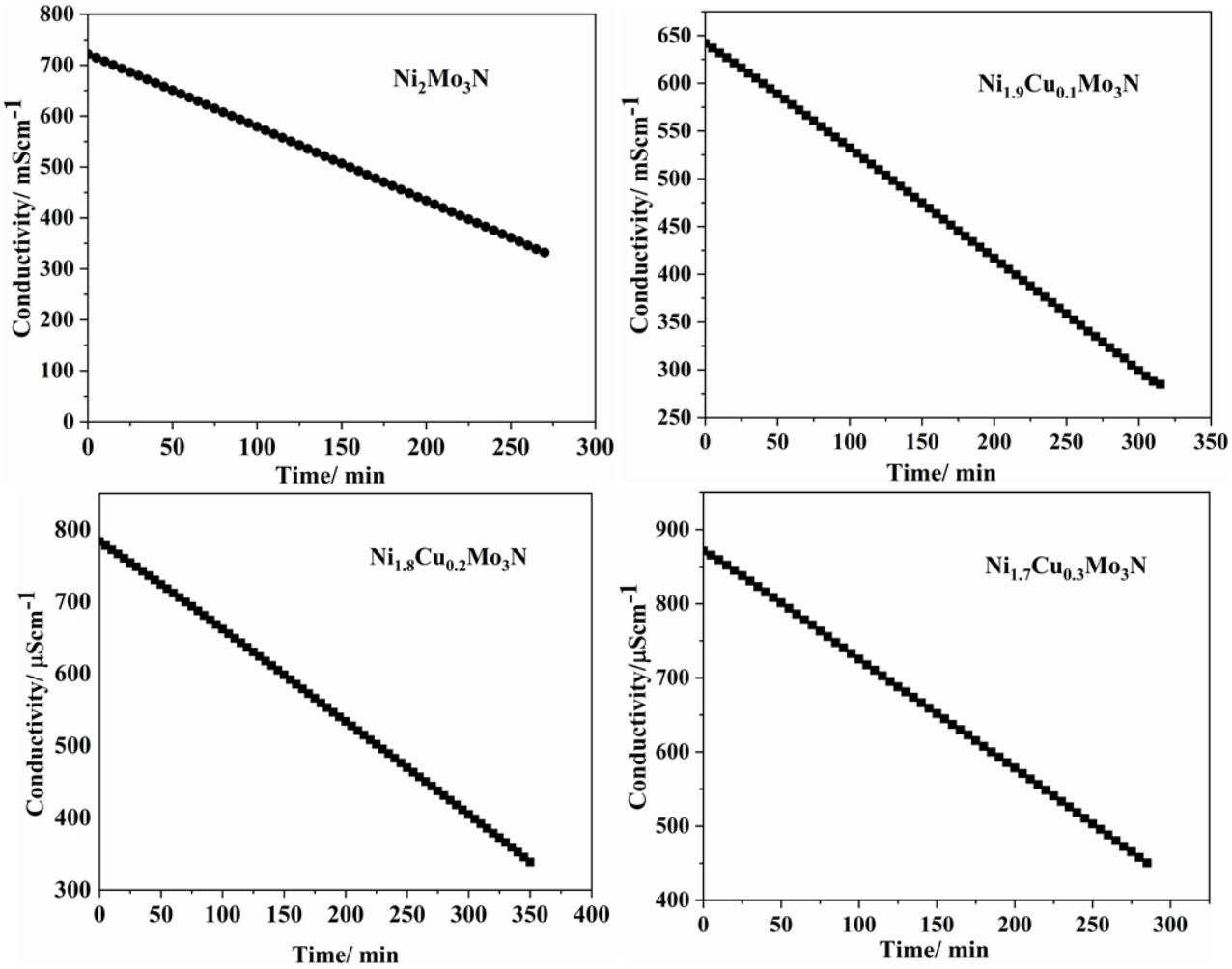

Fig. S16 Conductivity variation of the H_2SO_4 scrubber placed after heated $(Ni,Cu)_2Mo_3N$ at 500 °C under 75 vol % H_2 in N_2 (BOC, 99.98 %).

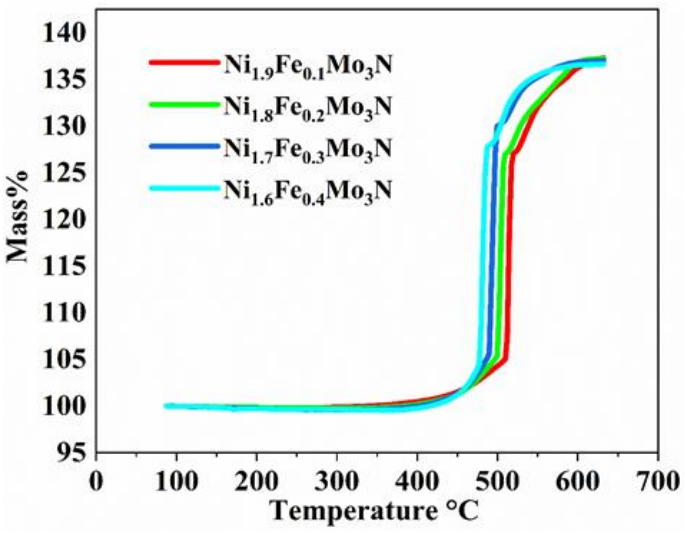

Fig. S17 Thermogravimetric analysis curves under 50% O_2/50% Ar atmosphere for the different Fe contents of $(Ni,Fe)_2Mo_3N$ (0, 0.1, 0.2 and 0.5) samples with the heating rate of 10 °C /min from room temperature to 700 °C. The initial weight of every sample before measurement is 0.015 g. Mass changes compared with calculated values are given in Table S5 and EDX data are given in Table S6.

Table S5 Mass % of various oxides formed from TGA of the resulting composites.

Composition	Overall Mass Gain Observed/%	Expected Mass Gain/ %
Ni_2Mo_3N	38.43	38.63
$Ni_{1.9}Fe_{0.1}Mo_3N$	37.45	38.61
$Ni_{1.8}Fe_{0.2}Mo_3N$	37.59	38.68
$Ni_{1.7}Fe_{0.3}Mo_3N$	37.13	38.71
$Ni_{1.6}Fe_{0.4}Mo_3N$	38.14	38.74

Table S6 The atom % of the Fe-doped Ni_2Mo_3N 900 °C samples evaluated by EDX analysis

Element	$Ni_{1.9}Fe_{0.1}Mo_3N$		$Ni_{1.7}Fe_{0.3}Mo_3N$		$Ni_{1.5}Fe_{0.5}Mo_3N$		$Ni_{1.2}Fe_{0.8}Mo_3N$	
	Calculated	Actual	Calculated	Actual	Calculated	Actual	Calculated	Actual
Ni	38	36	34	31.6	30	27.5	24	20
Fe	2	0.8	6	5	10	8.6	16	14
Mo	60	63	60	64	60	63	60	61

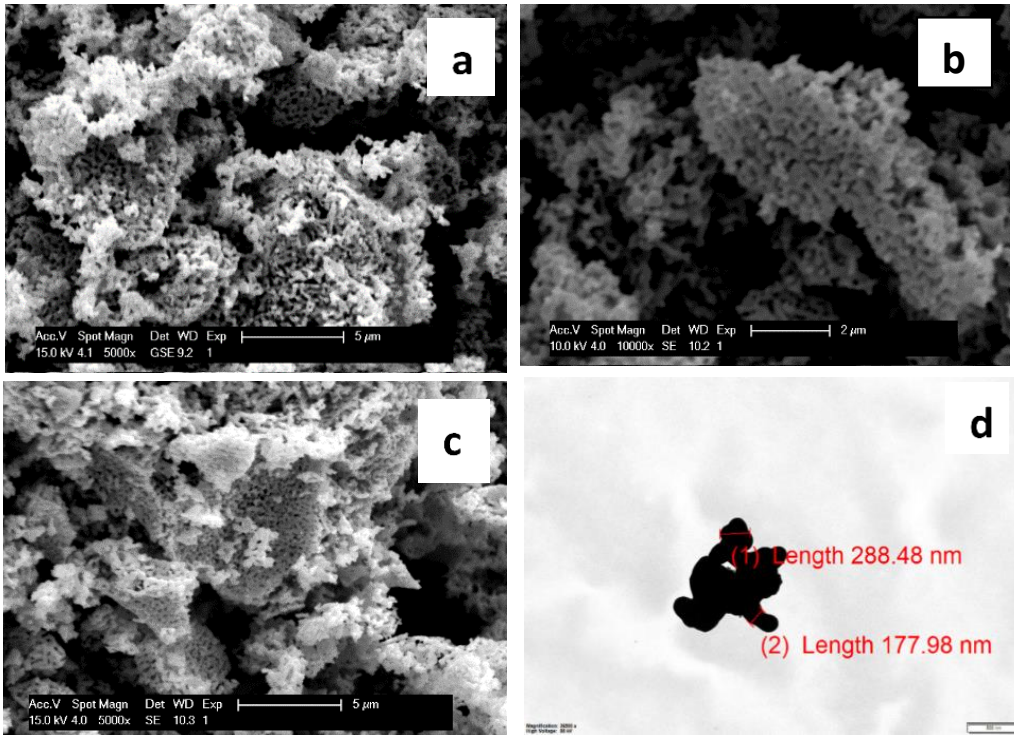

Fig. S18 SEM images (a), (b) and (c) of $Ni_{1.2}Fe_{0.8}Mo_3N$, $Ni_{1.6}Fe_{0.4}Mo_3N$ and $Ni_{0.8}Fe_{1.2}Mo_3N$ respectively. (d) TEM image of the fresh $Ni_{1.7}Fe_{0.3}Mo_3N$ catalyst.

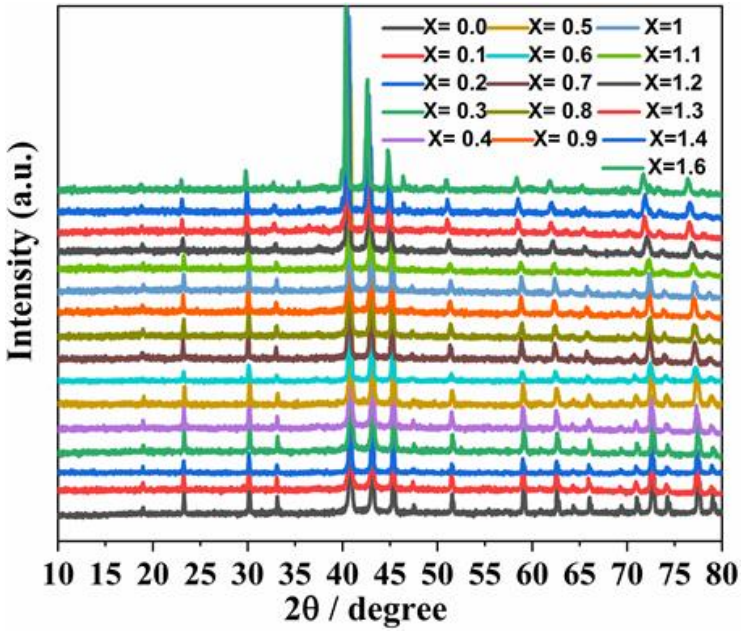

Fig. S19 XRD patterns of $Ni_{1-x}Fe_xMo_3N$ samples heated under NH_3 at 900 °C for 12 hr.

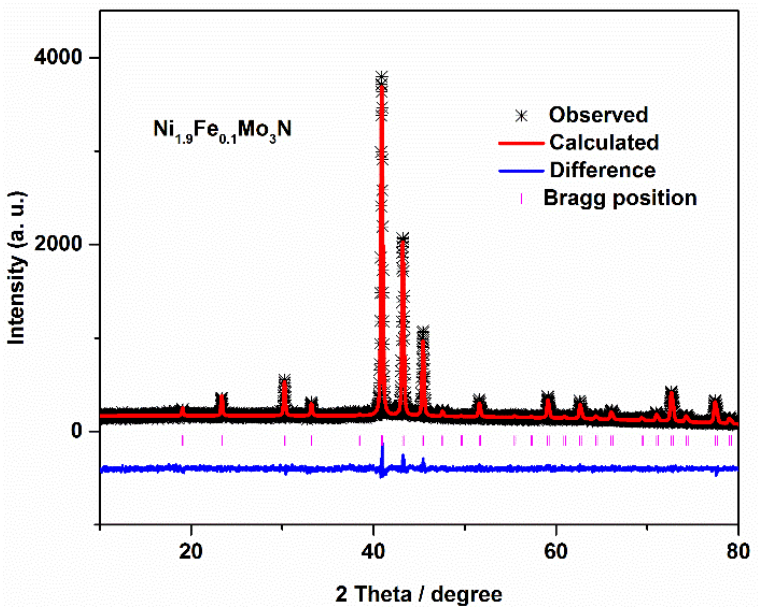

Fig. S20 Rietveld fit to the XRD data of $Ni_{1.9}Fe_{0.1}Mo_3N$. Black crosses mark the data points, the red continuous line the fit and the blue continuous line the difference. Pink tick marks show the positions of the allowed reflections for the filled β-manganese structure in $P4_132$ (Rp = 4.88 %, Rwp = 6.15 %, lattice parameter= 6.6369(2) Å.

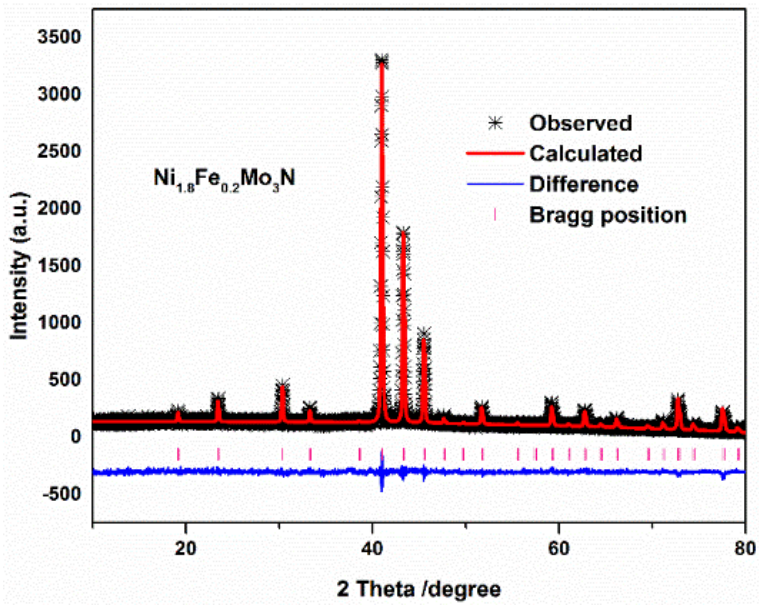

Fig. S21 Rietveld fit to the XRD data of $Ni_{1.8}Fe_{0.2}Mo_3N$. Black crosses mark the data points, the red continuous line the fit and the blue continuous line the difference. Pink tick marks show the positions of the allowed reflections for the filled β-manganese structure in $P4_132$ (Rp = 5.88 %, Rwp = 7.51 %, lattice parameter= 6.640192 (2) Å

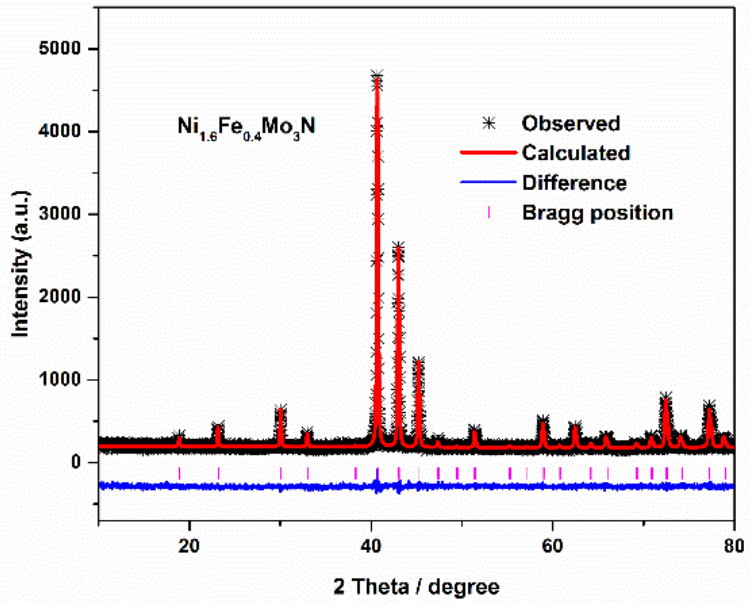

Fig. S22 Rietveld fit to the XRD data of $Ni_{1.6}Fe_{0.4}Mo_3N$. Black crosses mark the data points, the red continuous line the fit and the blue continuous line the difference. Pink tick marks show the positions of the allowed reflections for the filled β-manganese structure in $P4_132$ (Rp = 6.22 %, Rwp = 7.77 %, lattice parameter= 6.650198(2) Å.

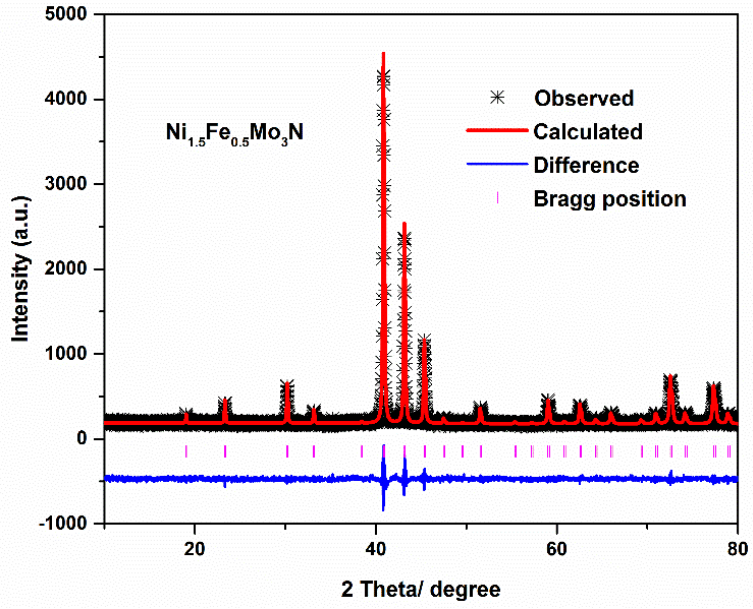

Fig. S23 Rietveld fit to the XRD data of $Ni_{1.5}Fe_{0.5}Mo_3N$. Black crosses mark the data points, the red continuous line the fit and the blue continuous line the difference. Pink tick marks show the positions of the allowed reflections for the filled β-manganese structure in $P4_132$ (Rp = 5.92 %, Rwp = 7.48 %, lattice parameter= 6.65553(2) Å.

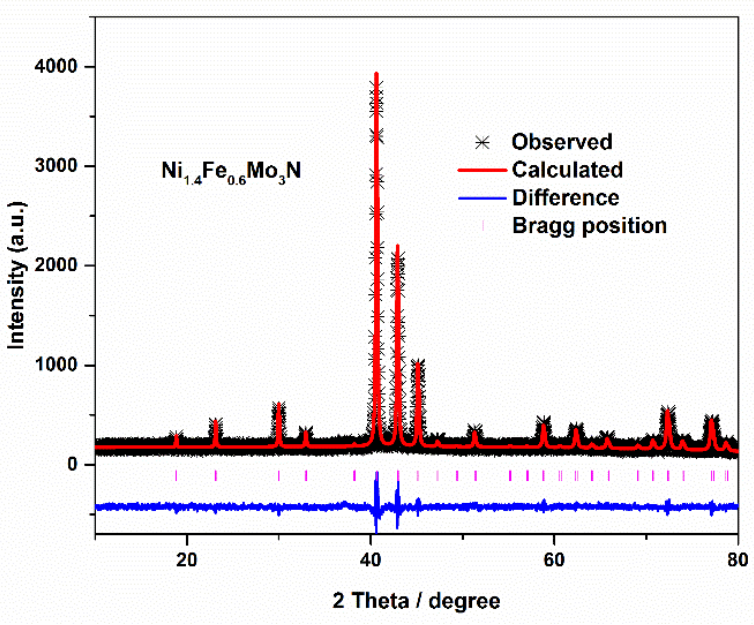

Fig. S24 Rietveld fit to the XRD data of $Ni_{1.4}Fe_{0.6}Mo_3N$. Black crosses mark the data points, the red continuous line the fit and the blue continuous line the difference. Pink tick marks show the positions of the allowed reflections for the filled β-manganese structure in $P4_132$ (Rp = 7.95 %, Rwp = 10.8 %, lattice parameter= 6.659(4) Å.

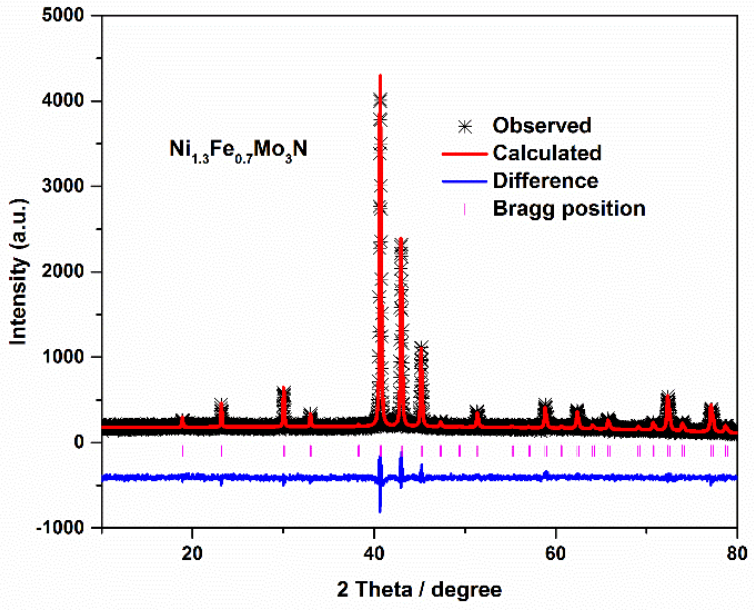

Fig. S25 Rietveld fit to the XRD data of $Ni_{1.3}Fe_{0.7}Mo_3N$. Black crosses mark the data points, the red continuous line the fit and the blue continuous line the difference. Pink tick marks show the positions of the allowed reflections for the filled β-manganese structure in $P4_132$ (Rp = 6.46 %, Rwp = 8.15 %, lattice parameter= 6.662(3) Å.

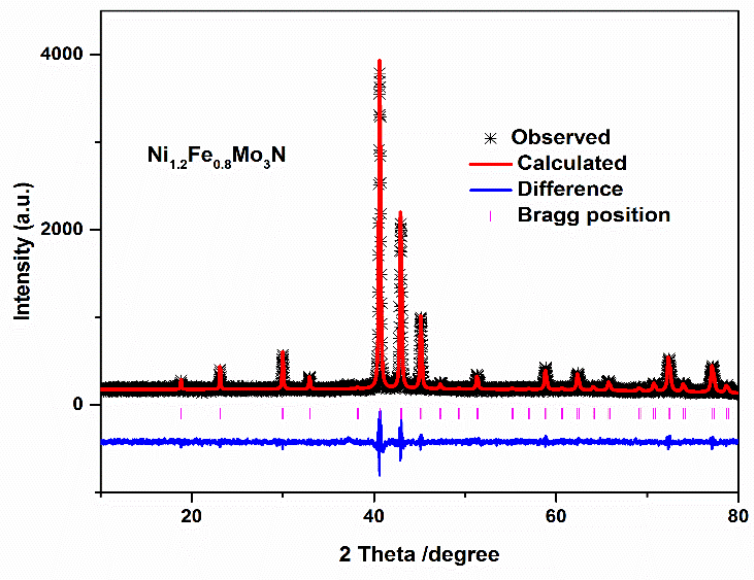

Fig. S26 Rietveld fit to the XRD data of $Ni_{1.2}Fe_{0.8}Mo_3N$. Black crosses mark the data points, the red continuous line the fit and the blue continuous line the difference. Pink tick marks show the positions of the allowed reflections for the filled β-manganese structure in $P4_132$ (Rp = 6.01 %, Rwp = 7.58 %, lattice parameter= 6.666(1) Å.

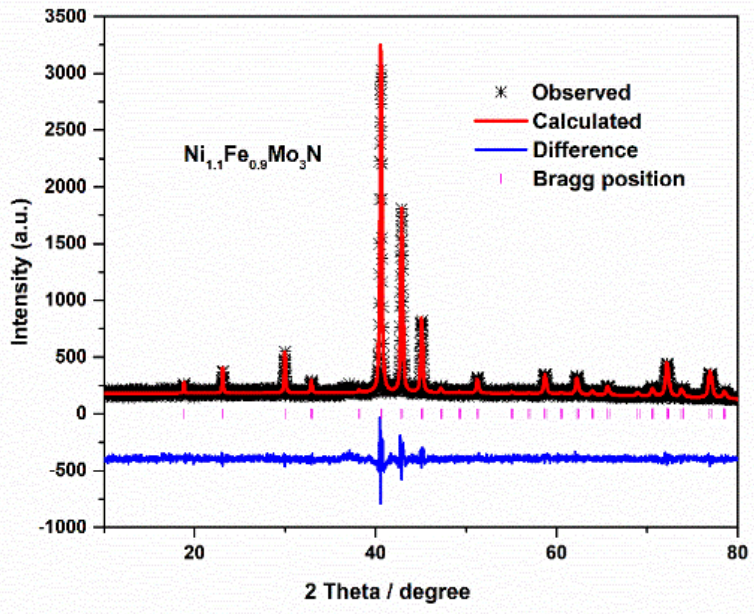

Fig. S27 Rietveld fit to the XRD data of $Ni_{1.1}Fe_{0.9}Mo_3N$. Black crosses mark the data points, the red continuous line the fit and the blue continuous line the difference. Pink tick marks show the positions of the allowed reflections for the filled β-manganese structure in $P4_132$ (Rp = 7.04 %, Rwp = 8.84 %, lattice parameter= 6.67298(5) Å.

Table S7 Structure information from Rietveld fits for $Ni_{2-x}Fe_x Mo_3N$ series.

Composition	a/Å	Ni/ Fe x (8c x, x, x)	Ni/ Fe Uiso / Å²	Mo 12 d (1/8, y, z)			N 4a 3/8, 3/8, 3/8
				y	Z	Uiso/ Å²	Uiso / Å²
Ni_2Mo_3N	6.6364(1)	0.0663(2)	0.0262(8)	0.20176(1)	0.45176(1)	0.02668(5)	
$Ni_{1.9}Fe_{0.1}Mo_3N$	6.63698(2)	0.06692(3)	0.026(1)	0.2019(1)	0.4519	0.024	
$Ni_{1.8}Fe_{0.2}Mo_3N$	6.64193(1)	0.06695(4)	0.0154(2)	0.20165(2)	0.45165	0.0127(1)	
$Ni_{1.7}Fe_{0.3}Mo_3N$	6.64765(3)	0.0672(4)	0.04385 (2)	0.20222(2)	0.45222	0.04376 (1)	
$Ni_{1.6}Fe_{0.4}Mo_3N$	6.650198(3)	0.067704(3)	0.0322(2)	0.20246(2)	0.45246	0.0271(1)	
$Ni_{1.5}Fe_{0.5}Mo_3N$	6.65532(2)	0.06778(4)	0.02688(1)	0.2025(2)	0.4525	0.010274(1)	0.2500
$Ni_{1.4}Fe_{0.6}Mo_3N$	6.65905(4)	0.068364(5)	0.01862(2)	0.202472(3)	0.45472	0.01887(1)	
$Ni_{1.3}Fe_{0.7}Mo_3N$	6.664 (3)	0.068439(6)	0.0304(2)	0.20307(2)	0.45307(1)	0.03188(1)	
$Ni_{1.2}Fe_{0.8}Mo_3N$	6.66784 (5)	0.067652(5)	0.048330(2)	0.203614(3)	0.45614	0.04304(2)	
$Ni_{1.1}Fe_{0.9}Mo_3N$	6.67298 (5)	0.067666(5)	0.042884(2)	0.20284 (2)	0.4584	0.042553(2)	
$NiFeMo_3N$	6.6812 (5)	0.054013(4)	0.0154(2)	0.20355(2)	0.4555	0.026(1)	

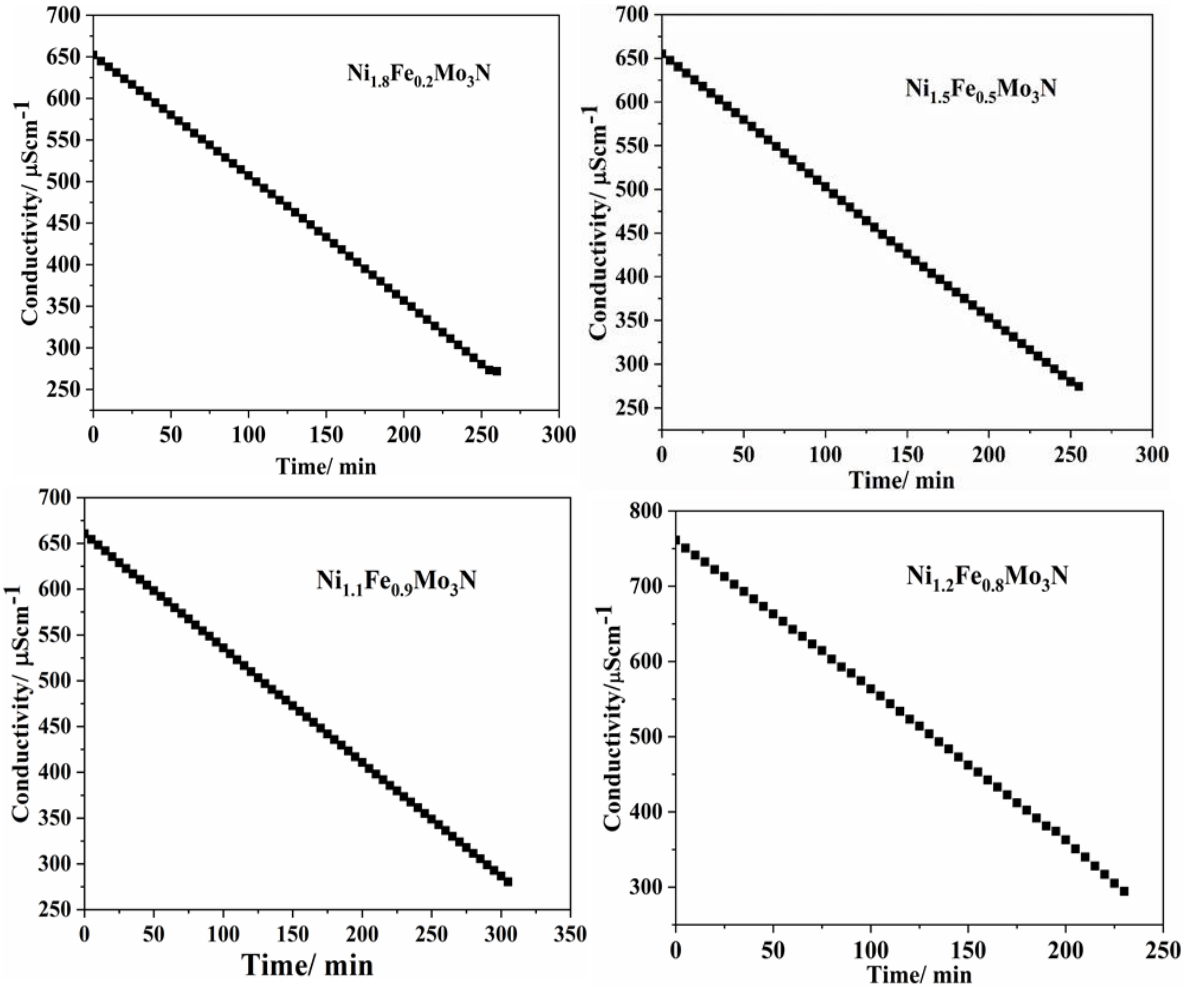

Fig. S28 Conductivity of the H_2SO_4 scrubber placed after heated $(Ni,Fe)_2Mo_3N$ at 500 °C under 75 vol % H_2 (BOC, 99.998 %) in N_2 (BOC, 99.995 %).

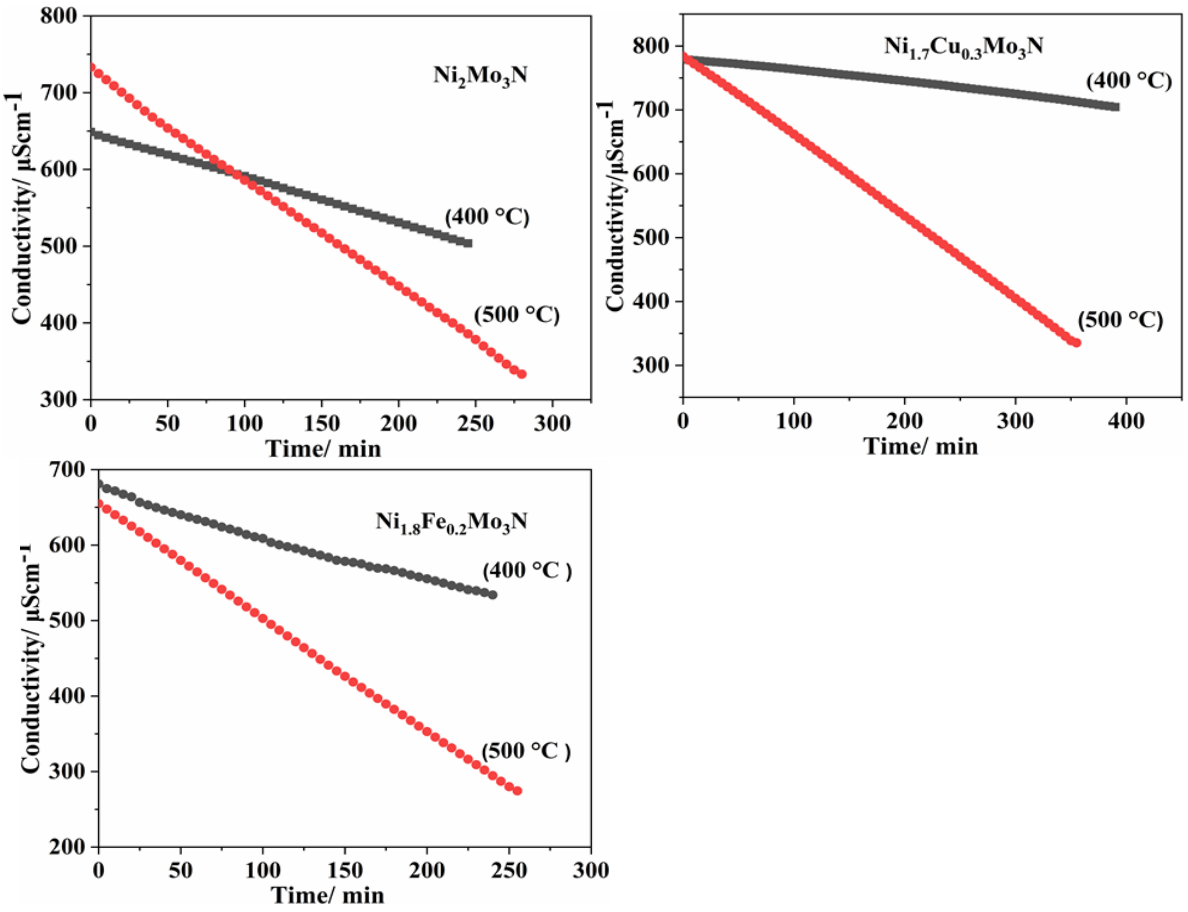

Fig. S29 Comparison of ammonia synthesis reaction profiles for Ni_2Mo_3N (A), $Ni_{1.7}Cu_{0.3}Mo_3N$ (B) and $Ni_{1.8}Fe_{0.2}Mo_3N$ (C) under 75 vol % H_2 in N_2 (BOC, 99.98%) at 400 and 500 °C.

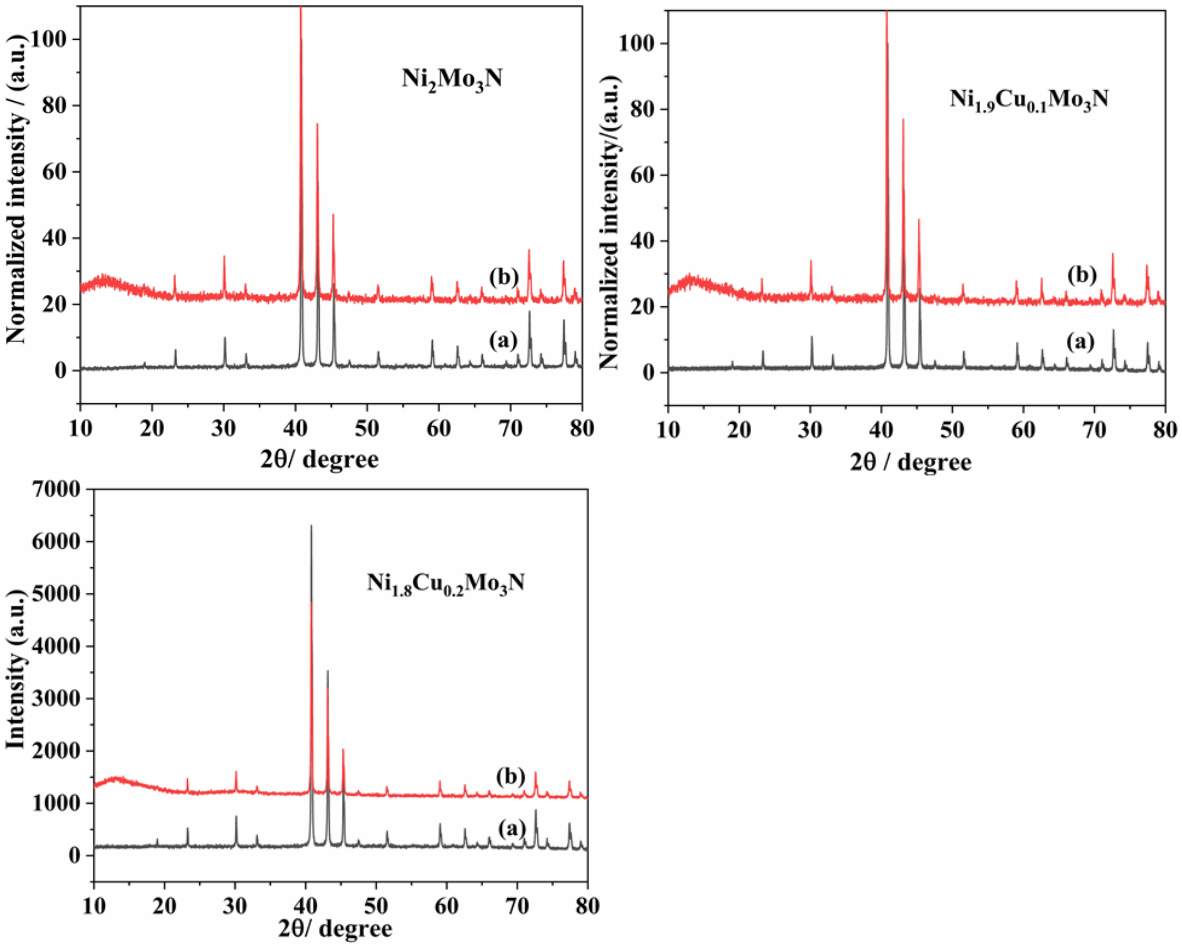

Fig. S30 XRD patterns collected for (a) pre-reaction and (b) post-reaction of $Ni_{1.9}Cu_{0.1}Mo_3N$ (left) and $Ni_{1.8}Cu_{0.2}Mo_3N$ (right).

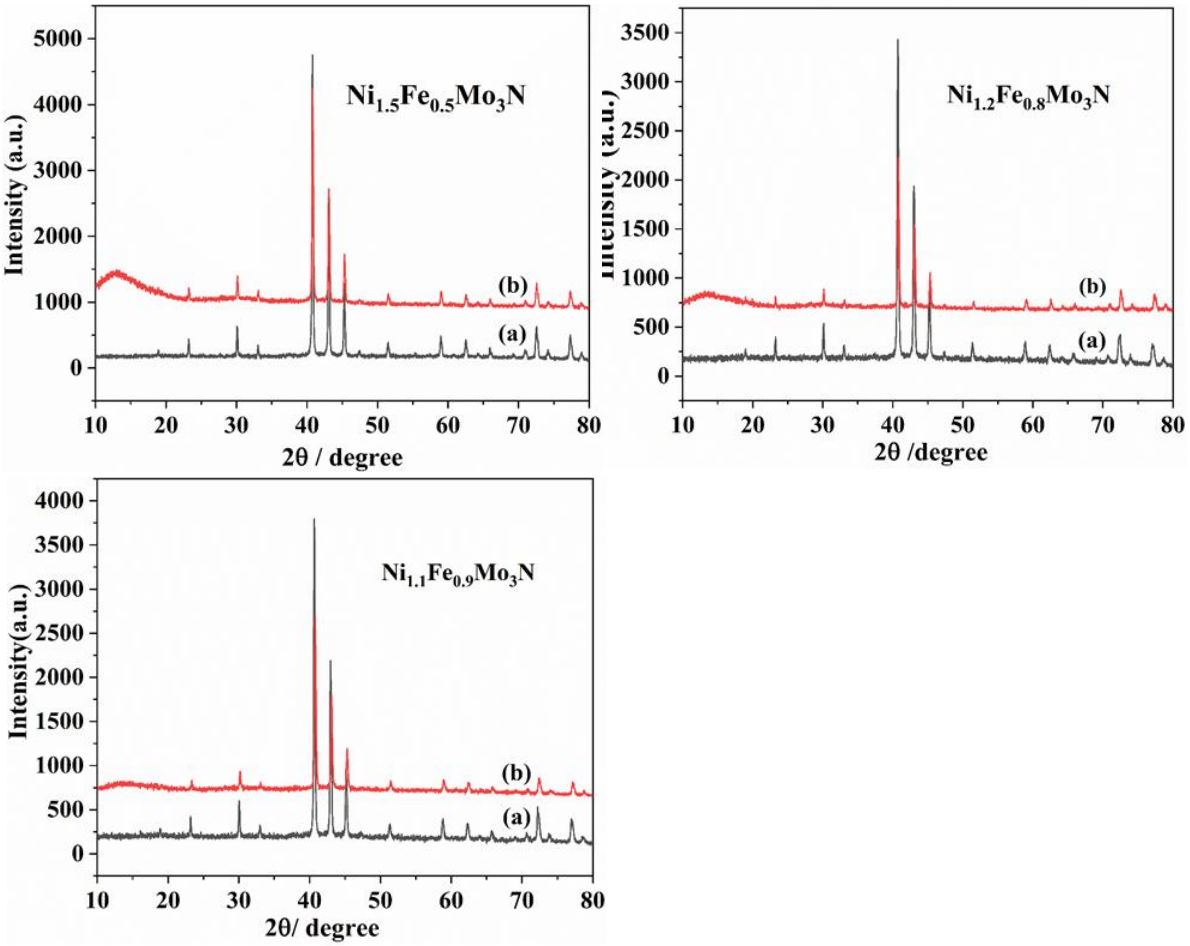

Fig. S31 PXRD patterns collected for (a) pre-reaction and (b) post-reaction of $Ni_{1.5}Fe_{0.5}Mo_3N$, $Ni_{1.2}Fe_{0.8}Mo_3N$ and $Ni_{1.1}Fe_{0.9}Mo_3N$.

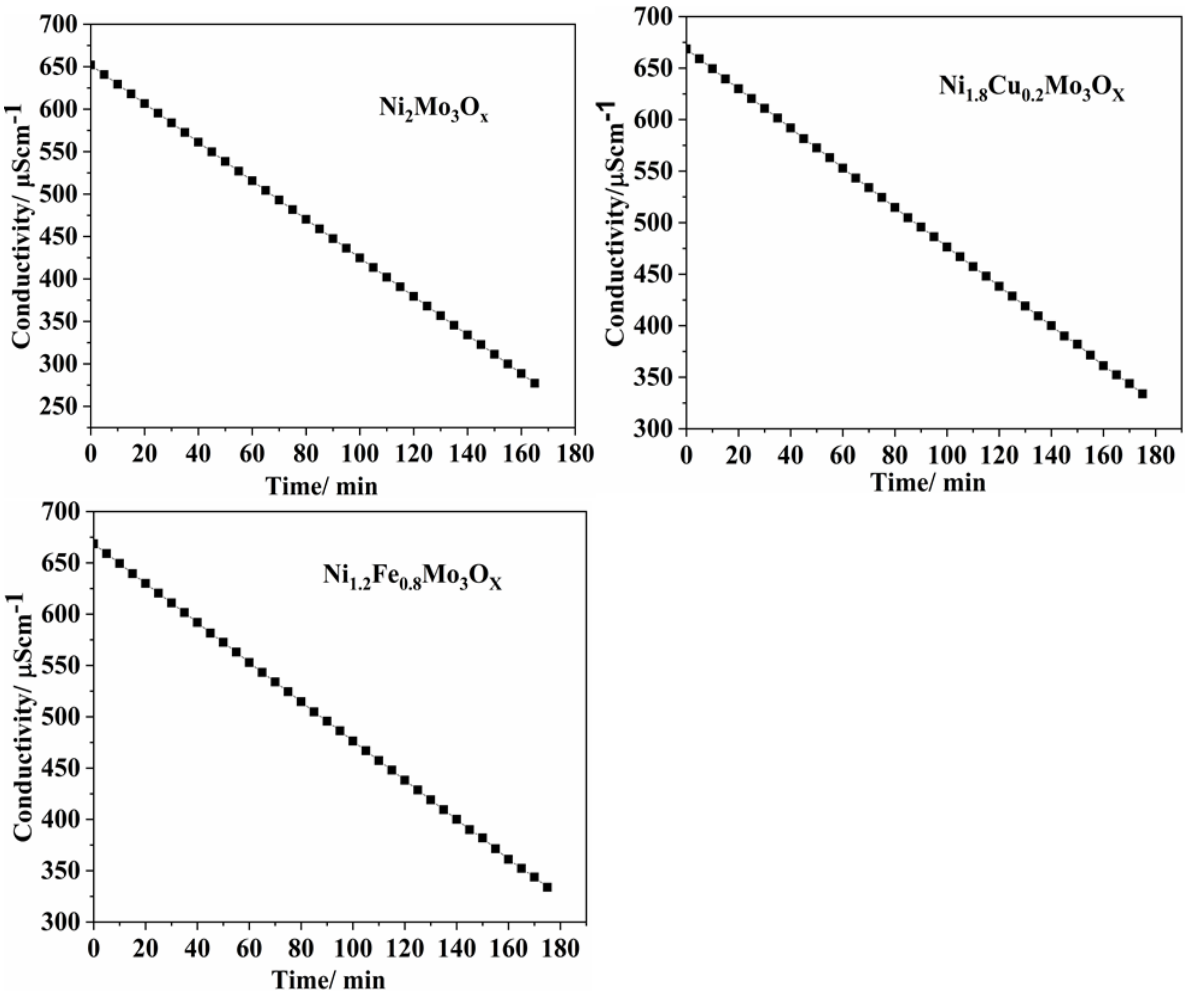

Fig. S32 Conductivity of the H_2SO_4 scrubber placed after heated $Ni_2Mo_3O_X$, $Ni_{1.7}Cu_{0.3}Mo_3O_X$ and $Ni_{1.2}Fe_{0.8}Mo_3O_X$ at 500 °C under 75 vol % H_2 (BOC, 99.998 %) in N_2 (BOC, 99.995 %). These catalyst samples were prepared during the catalyst activation step.